Phototransduction in transgenic mice after targeted deletion of the rod transducin α-subunit

P. D. Calvert*†, N. V. Krasnoperova†‡, A. L. Lyubarsky†§, T. Isayama*, M. Nicoló‡, B. Kosaras¶, G. Wong‖, K. S. Gannon‖, R. F. Margolskee‖, R. L. Sidman¶, E. N. Pugh, Jr.§, C. L. Makino*,**, and J. Lem††

* Department of Ophthalmology, Harvard Medical School and the Massachusetts Eye and Ear Infirmary, Boston, MA 02114; ‡Department of Ophthalmology and Molecular Cardiology Research Institute, New England Medical Center, Boston, MA 02111; §Department of Ophthalmology and Institute for Neurological Sciences, University of Pennsylvania, Philadelphia, PA 19104; ‖Howard Hughes Medical Institute, Department of Physiology and Biophysics, Mount Sinai School of Medicine, New York, NY 10029; ¶Department of Neurosurgery, Brigham and Women's Hospital, Harvard Medical School, Boston, MA 01772; and ††Department of Ophthalmology and Program in Genetics, Tufts University School of Medicine, Boston, MA 02111

Contributed by R. L. Sidman, October 9, 2000

Retinal photoreceptors use the heterotrimeric G protein transducin to couple rhodopsin to a biochemical cascade that underlies the electrical photoresponse. Several isoforms of each transducin subunit are present in the retina. Although rods and cones seem to contain distinct transducin subunits, it is not known whether phototransduction in a given cell type depends strictly on a single form of each subunit. To approach this question, we have deleted the gene for the rod transducin α-subunit in mice. In hemizygous knockout mice, there was a small reduction in retinal transducin α-subunit content but retinal morphology and the physiology of single rods were largely normal. In homozygous knockout mice, a mild retinal degeneration occurred with age. Rod-driven components were absent from the electroretinogram, whereas cone-driven components were retained. Every photoreceptor examined by single-cell recording failed to respond to flashes, with one exception. The solitary responsive cell was insensitive, as expected for a cone, but had a rod-like spectral sensitivity and flash response kinetics that were slow, even for rods. These results indicate that most if not all rods use a single transducin type in phototransduction.

In vertebrate retinal rods, photoexcited rhodopsin activates the G protein transducin which promotes cGMP hydrolysis by phosphodiesterase (PDE). The fall in intracellular cGMP results in the closure of ion channels in the outer segment and, subsequently, membrane hyperpolarization (reviewed in ref. 1). Retinal cones, which are less sensitive than rods, use a similar G protein cascade in phototransduction but with a distinct set of proteins. The subunit composition of cone transducin differs entirely from that of rods. Rod transducin consists of transducin α-subunit (Trα), Gβ1, and Gγ1, whereas cone transducin is composed of Tcα, Gβ3, and Gγc (2–7). In addition, Gγ2 localizes to cone outer segments (6), although it does not interact strongly with Gβ3 (8, 9). Little is known about the significance of transducin-subunit diversity. Moreover, it is unclear whether the cell specificity of expression is absolute. To explore functional specificity, the Trα gene was knocked out in mice. Photoreceptor function was assessed by electroretinogram (ERG) recordings that monitor the massed-field potential across the retina and from suction electrode recordings of individual photoreceptors.

Materials and Methods

Knockout Mouse Construction. The Trα gene was cloned from a 129SV genomic library (Stratagene) and used to produce the targeting vector shown in Fig. 1*A*. The targeting vector was introduced into the W9.5 embryonic stem cell line as described by Kwee *et al.* (10). Of 308 clones collected, 115 were tested by Southern blot analysis, and 20 were identified as homologously recombinant by using one of two restriction-digestion strategies. Proper identification was verified in 4 of 10 clones by using both restriction-digestion strategies (Fig. 1*A*). Three of these clones were injected into BALB/c blastocysts to produce chimeric founders. Founders were crossed with BALB/c mice, and pigmented Trα hemizygous knockout (Trα +/−) offspring were bred to homozygosity.

Knockout was confirmed at the DNA level by Southern blot analysis essentially as described in Lem *et al.* (11). Briefly, 6 μg of genomic DNA was digested with *Xba*I (New England Biolabs), run on a 0.5% agarose gel, transferred to nylon membrane, and UV cross-linked. Blots were prehybridized in 50% (vol/vol) formamide/0.5 M Na_2HPO_4/1 mM EDTA/1% BSA/5% (vol/vol) SDS and probed with a 1.6-kb fragment of heat-denatured, double-stranded DNA that was radiolabeled by random priming with [^{32}P]dATP. After overnight hybridization, blots were washed at high stringency with 2× SSC/0.1% SDS at 65°C and 0.1× SSC/0.1% SDS at 65°C. Membranes were exposed to Kodak XAR film for 1–4 days.

Messenger RNA levels were measured by the reverse transcription–PCR of DNA prepared from retinas of 4-week-old Trα homozygous knockout (Trα −/−) mice. The cDNA was analyzed by using the Trα N-terminus primer pairs (5′–3′): GCCAGCGCTGAGGAGAAGCAC and CCAG/ATACCCGTCCTGGTGGAT. The annealing temperature was ramped from 65 to 55°C with an extension temperature of 72°C for 35 cycles. The C-terminal primers were: GAGGGTGTGACGTGCATCATTTT and GCCGGCATCCTCGTAAGTGTTA. The annealing temperature was ramped from 68 to 62°C with an extension temperature of 72°C for 35 cycles. The primers for rhodopsin were TACATCCCTGAGGGCATGCAA and TCAACATGATGTAGATGACCGG, and were used for annealing at 61°C with an extension temperature of 72°C for 35 cycles.

Determination of Protein Content. Rhodopsin was extracted from the retinas of 5- to 8-week-old Trα −/−, Trα +/−, and littermate-control mice in 30 mM cetyltrimethylammonium chloride (Fluka) and then quantified by taking difference spectra with an extinction coefficient of 40,600 liters·mol^{-1}·cm^{-1} (12). For the analysis of other proteins, retinas from mice aged 4–9 weeks were harvested into ice-cold buffer containing (in mM): 130 NaCl/2.6 KCl/2.4 $MgCl_2$/1.2 $CaCl_2$/10 Hepes/0.02 EDTA, pH 7.4 and frozen at −70°C. After thawing, the retinas were homogenized in hypotonic buffer containing (in mM): 10

Abbreviations: ERG, electroretinogram; PDE, phosphodiesterase; WT, wild type.

†P.D.C., N.V.K., and A.L.L. contributed equally to this study.

**To whom reprint requests should be addressed at: Department of Ophthalmology, Harvard Medical School, 243 Charles Street, Boston, MA 02114. E-mail: cmakino@meei.harvard.edu.

The publication costs of this article were defrayed in part by page charge payment. This article must therefore be hereby marked "*advertisement*" in accordance with 18 U.S.C. §1734 solely to indicate this fact.

Article published online before print: *Proc. Natl. Acad. Sci. USA*, 10.1073/pnas.250478897. Article and publication date are at www.pnas.org/cgi/doi/10.1073/pnas.250478897

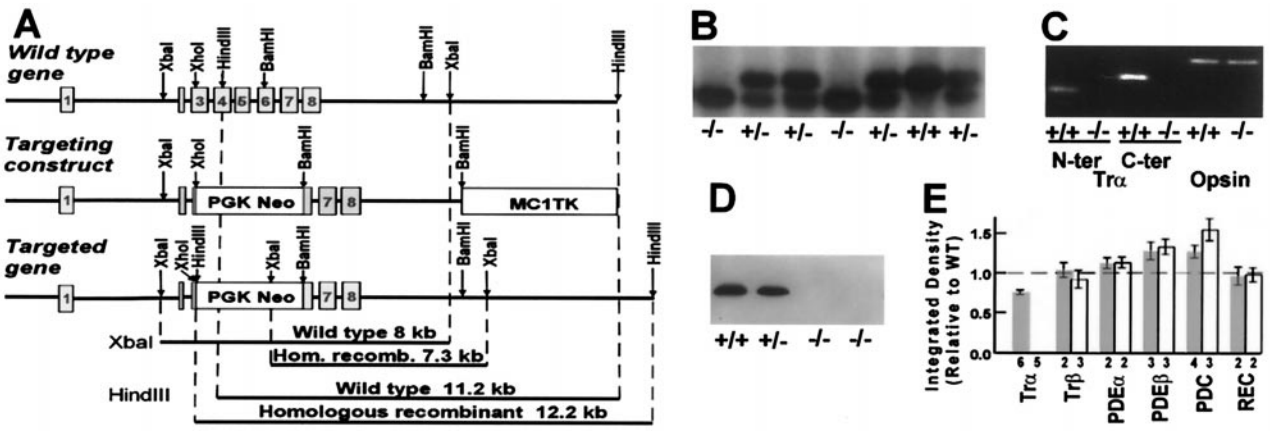

Fig. 1. Molecular characterization of Trα $-/-$ mice. (*A*) Gene-targeting strategy for knocking out Trα. Codons 63–207 of the wild-type (WT) Trα gene (top) were deleted by replacing the sequence between the *Xho*I site in exon 3 and the *Bam*HI site in exon 6 with the phosphoglycerate kinase-driven neomycin resistance (PGK Neo) gene. The thymidine kinase gene MC1TK was attached to the 3′ end of the targeting construct for use in a negative-selection strategy. Diagnostic *Xba*I or *Hin*dIII restriction digestions distinguished the homologous recombinant (Hom. recomb.) from the WT gene. (*B*) Southern blot of *Xba*I digested DNA from tail samples of three litters of mice. Trα alleles from WT and Trα $-/-$ appeared as 8- and 7.3-kb fragments, respectively. (*C*) Absence of Trα mRNA in Trα $-/-$ retinas. Trα transcripts were not detected in Trα $-/-$ mice by reverse transcription–PCR with primers specific for either the N or C terminus of the gene. The same procedure gave a positive result in littermate controls. Rod opsin expression was detected in both control and knockout mice by using rod opsin-specific PCR primers. Genotypes and PCR primers are shown at the bottom. (*D*) Lack of Trα protein in Trα $-/-$ retinas. In the Western analysis, Trα was labeled by mab 4A in WT and Trα $+/-$ mice but not in littermate-Trα $-/-$ mice even after loading 50 times more homogenate onto the gel (far right). (*E*) Altered amounts of Trα, PDE, and phosducin in retinas of Trα $+/-$ (gray bars) and Trα $-/-$ (open bars) mice as determined by Western analysis. Error bars denote SEM. The numbers of determinations are listed below the histogram.

Tris·HCl/2 DTT/2 EDTA/1 benzamidine/0.1 phenylmethylsulfonyl fluoride and 15 mg·ml^{-1} each of aprotinin, leupeptin, and pepstatin (pH 7.4). Homogenates were solubilized in 2% (vol/vol) SDS and centrifuged at 10,000 $\times$ *g*. Proteins were separated by electrophoresis on 12.5% polyacrylamide gels and transferred onto nitrocellulose membranes for 1–1.5 h. After blocking with 5% (vol/vol) nonfat dried milk/0.05% Tween 20 (J. T. Baker)/150 mM NaCl/100 mM Tris·HCl, pH 7.4 membranes were probed with primary antibodies raised against: Trα, Mab 4A (N-terminus; ref. 13), and Tα1A (amino acids 85–103; a gift from M. Lochrie and M. Simon, California Institute of Technology, Pasadena); rod transducin β-subunit, β-636 (5); PDEα- and PDEβ-subunits, Pat (a gift from R. Lee, University of California, Los Angeles); phosducin, Gertie B (14); and recoverin, P26 (15). Antibodies were visualized by enhanced chemiluminescence and x-ray film. Integrated band density was quantified by using Scanalytics 2DGEL software (Billerica, MA).

Histology. Anesthetized mice were perfused with freshly prepared 2% (vol/vol) paraformaldehyde/2.5% glutaraldehyde in 0.1 M phosphate buffer, pH 7.4. Eyes were exenterated, rinsed with buffer, and placed into 2% (vol/vol) osmium tetroxide. The globe was hemisected along the vertical meridian, dehydrated, and embedded in Epon. Sections that were 1 μm thick were stained with alkaline toluidine blue for light microscopy.

Electroretinography. Mice were maintained and ERGs were recorded as described in Lyubarsky *et al.* (16). WT mice consisted of three mice from the Tufts colony and three C57BL mice from Charles River Breeding Laboratories. Before an experiment, 8- to 10-week-old mice were dark adapted for 12–20 h, anesthetized with (in μg·g^{-1} of body weight): 25 ketamine, 10 xylazine, and 1,000 urethane, and their pupils were dilated with 1% tropicamide saline (Mydriacil, Alconox, New York). A platinum wire in contact with the cornea through methylcellulose was used as a recording electrode, whereas a tungsten needle inserted into the forehead served as a reference. Preparations were carried out in dim red light, after which the animal was placed in complete darkness for 10 min before initiation of the recording session. Ganzfeld illumination was provided either by an array of three xenon arc sources (Mouser Electronics, Randolph, NJ) that delivered >85% of their energy in 1 ms or by a halogen lamp (HLX 64610, Osram, Berlin). Exposure duration was controlled by an electronic shutter. The light was not collimated at the interference filters (Ealing Electrooptics, Holliston, MA); thus, the spectral output was broadband although centered slightly to the short-wavelength side of the nominal wavelength of the filter. The effective wavelength of the stimuli was determined as described by Lyubarsky *et al.* (16). The stimulus intensities were converted into amount of rhodopsin or cone pigment photoisomerized as described (16–18).

Single-Cell Physiology. Trα $-/-$, Trα $+/-$, and littermate control mice, aged 5–10 weeks, were dark adapted overnight, anesthetized with CO_2, and killed by cervical dislocation. Tissue was prepared for recording (19) under infrared light. Small samples of retina were chopped finely in Leibovitz's L-15 (GIBCO) supplemented with DNase I (type IV, Sigma), placed in an experimental chamber, and perfused continuously. The perfusion solution, containing (in mM) 144 Na^+, 3.6 K^+, 1.2 Ca^{2+}, 2.4 Mg^{2+}, 123.3 Cl^-, 10 Hepes, 20 HCO_3^-, 0.02 EDTA, 10 glucose, 0.5 glutamate, 3 succinate, BME vitamins, MEM amino acids (pH 7.4), was equilibrated with 95% O_2/5% CO_2 and heated to 36–38°C. An outer segment was pulled into a glass electrode, and the circulating current was recorded with a current-to-voltage converter (Axopatch 200A, Axon Instruments, Foster City, CA). The electrode was filled with a solution similar to that used for perfusion, except that HCO_3^- was replaced with equimolar Cl^-, and vitamins and amino acids were omitted. Rods were stimulated with light from a shuttered xenon-arc source. The spectral composition was controlled with interference filters with bandwidths at half-maximal transmission that were nominally 10 nm (Omega Optical, Brattleboro, VT). Records were low-pass filtered (30 Hz, -3 dB, 8-pole Bessel) then digitized at 400 Hz. No corrections were made for delays introduced by low-pass filtering. Additional digital filtering at 7 Hz was achieved by convolution with a Gaussian. Spectral sensitivity was found from the wavelength dependence of relative flash sensitivity. After suc-

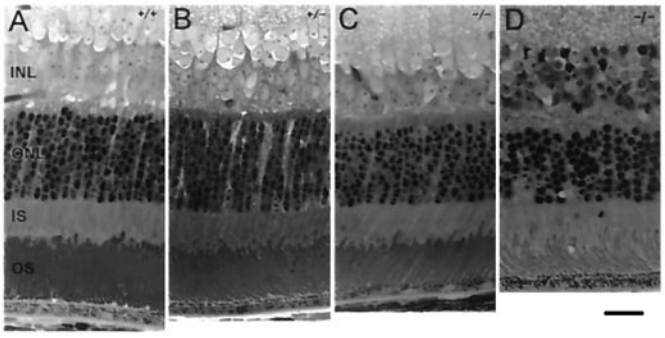

Fig. 2. Retinal morphology at 4 weeks. (*A*) Trα +/+. (*B*) Trα +/−. (*C*) Trα −/−. (*D*) Trα −/− at 51 weeks. INL, inner nuclear layer; ONL, outer nuclear layer; IS, inner segments; OS, outer segments. (bar = 20 μm.)

cessful recordings, ejection of WT rods from the electrode sometimes disrupted the outer segment structure because of the tightness of the seal. To minimize the possibility of damage to Trα −/− cells, oversized electrodes were sometimes used. Nonetheless, only Trα −/− cells whose outer segments remained intact after ejection from the electrode were tallied.

Results

The Trα gene was disrupted by replacement of exons 4 and 5 and parts of exons 3 and 6 with the PGK Neo gene (Fig. 1*A*). Germ-line transmission of the disrupted gene was verified by Southern blot analysis (Fig. 1*B*). Trα mRNA was detected by reverse transcription–PCR in WT and Trα +/− retinas but not in Trα −/− retinas (Fig. 1*C*). This result indicated that truncated protein was not produced. On further testing, Trα protein was not detected in Trα −/− retinas by Western analysis with either of two antibodies (Fig. 1 *D* and *E*). Thus, Trα was not expressed in Trα −/− mice. Trα +/− retinas contained ≈80% of WT levels of Trα, suggesting that rods could partially compensate for the loss of one allele (Fig. 1*E*).

Levels of several other phototransduction proteins were also examined. Difference spectrophotometry showed that Trα −/− (n = 2) and Trα +/− (n = 3) mice had a rhodopsin content of 0.4 nmol per retina, indistinguishable from that measured in WT mice (n = 2). Levels of Tβ and recoverin were also normal in Trα +/− and Trα −/− mice by Western analysis, but phosducin, PDEα-, and PDEβ-subunits may have been elevated slightly (Fig. 1*E*).

Although the gross morphology of the retina was largely unaffected by Trα deletion, there was some degeneration with age (Fig. 2). The outer nuclear layer consists of photoreceptor nuclei; thus, its thickness serves as a gauge for the number of rods present. At 4 weeks of age, outer-nuclear-layer thickness was similar in Trα +/− and controls, whereas in Trα −/−, it may have been slightly thinner. Outer-segment length seemed to be normal in both Trα +/− and Trα −/− mice. By 13 weeks, Trα −/− rod-outer-segment length had shortened, and the thickness of the outer nuclear layer had decreased by about one row of nuclei, indicating a loss of ≈10% of the rods. There was little further change in the Trα −/− outer nuclear layer or outer-segment length at 51 weeks, but the inner nuclear layer was somewhat thinner, perhaps as a result of the secondary loss of neurons downstream from the photoreceptors.

ERGs of WT and Trα −/− mice were recorded under conditions chosen to reveal various aspects of retinal function; examples are shown in Fig. 3*A*. As expected from previous investigations (20), flashes that produced only a few photoisomerizations per rod (trace a) elicited a prominent rod b-wave in dark-adapted WT mice. The rod b-wave is a massed potential

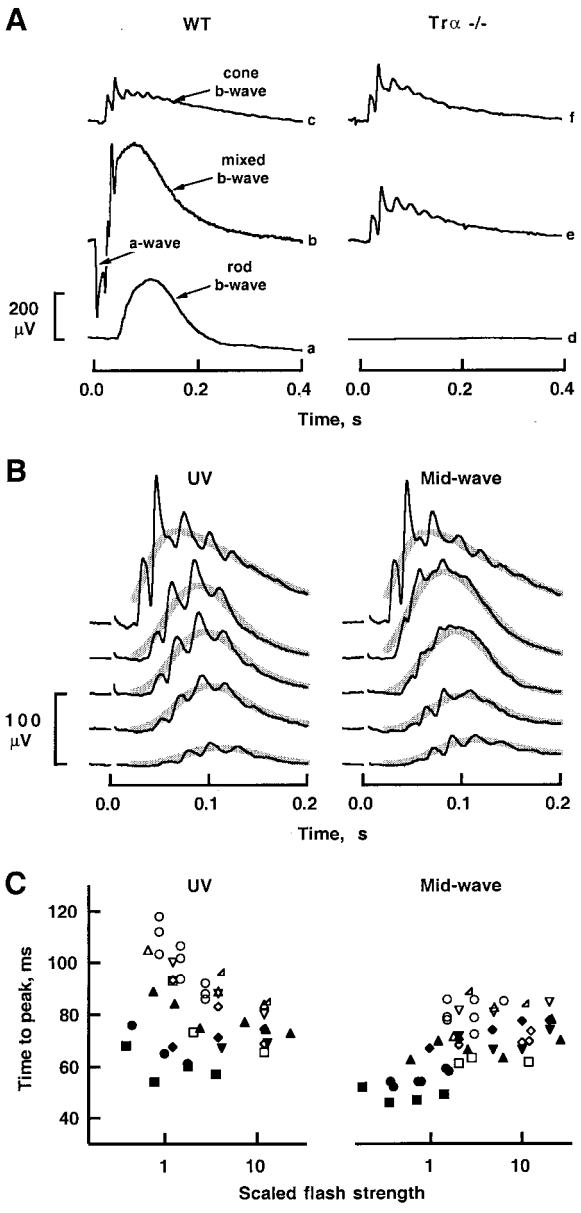

Fig. 3. ERGs of Trα −/− and WT mice. (*A*) Lack of rod-driven components in Trα −/− mice. Brief flashes of 513 nm, isomerizing 4.7 rhodopsin molecules per rod (traces a and d), or of white light isomerizing ≈530,000 rhodopsins per rod (traces b, c, e, and f), were delivered at time = 0 s. The white flashes also isomerized an estimated 0.087% of the UV-sensitive cone pigment and 1.2% of the mid-wavelength-sensitive cone pigment (16). Traces c and f were obtained in response to flashes superimposed on a 540-nm background light that isomerized ≈4,000 rhodopsins·rod^{-1}·s^{-1}. (*B*) Cone-driven b-waves elicited by UV (357 nm) and mid-wave (513 nm) flashes for a Trα −/− mouse in the absence of background light. Responses from 5–20 trials were averaged (black traces) and digitally filtered with a Gaussian filter (12 Hz, −3 dB; thick gray traces). Flashes delivered (bottom to top, in photons·μm^{-2} at the cornea): 1,200, 3,700, 6,280, and 11,700 at 357 nm and 4,300, 8,990, 22,100, 92,000, at 513 nm. Saturated responses (topmost in each column of responses) were elicited by bright, white flashes that isomerized ≈1.2% and ≈0.087% of the pigment in mid-wavelength- and UV-sensitive cones, respectively. (*C*) Dependence of cone b-wave time to peak on flash strength. UV (357) and mid-wave (513 nm) flashes were presented 2 s after the onset of the 540-nm background. Time to peak was taken as the interval between flash onset and the peak of the low-pass-filtered responses (see *B*) of WT (filled symbols) and Trα −/− (open symbols) mice. The flash intensities for each animal were scaled by the intensity that produced a 20% maximal response; thus, a scaled flash of unit intensity produced a b-wave whose amplitude was 20% of the saturated amplitude.

generated predominantly by rod-driven bipolar cells (20, 21). In contrast, Trα $-/-$ mice did not produce a detectable rod b-wave (trace d), indicating a major defect in the rods and/or in the rod bipolar cells. To characterize this defect further and to evaluate functionality of the cone-driven neurons, mice were stimulated by bright, white flashes that isomerized $\approx$1% of the rhodopsin. In dark-adapted WT mice, this stimulus elicited a characteristic, large (hundreds of microvolts), corneal-negative a-wave (trace b). Because the a-wave in mice is generated almost exclusively by suppression of the rod circulating current (16, 17, 20), its absence in Trα $-/-$ mice (trace e) established that the rod circulating current was absent or unresponsive to light. Dark-adapted Trα $-/-$ mice did nonetheless exhibit responses to intense flashes, but they consisted only of corneal-positive signals (trace e) that closely resembled the murine cone b-wave (16, 22). To test the cone origin of the Trα $-/-$ ERG, mice were exposed to a 540-nm background light that isomerized $\approx$4,000 rhodopsins$\cdot$rod$^{-1}\cdot$s^{-1}; in WT mice, this background suppresses over 95% of the rod circulating current (16). Superposition of the bright probe flash ($\approx$1% of rhodopsin isomerized) on this rod-saturating background gave rise to ERGs in WT and Trα $-/-$ mice that closely resembled each other (Fig. 3*A*, traces c and f) and that of the same, dark-adapted Trα $-/-$ mouse (trace e), supporting the hypothesis that the Trα $-/-$ responses originated from cone-driven cells.

The mouse retina contains UV- and mid-wave-sensitive cones and retinal neurons selectively driven by these cones (16). Functionality of the UV- and mid-wavelength-sensitive cone-driven neurons in Trα $-/-$ animals was tested by stimulation with UV (357 nm) and mid-wavelength (513 nm) flashes. Both UV and mid-wave stimuli were effective in eliciting ERGs (Fig. 3*B*). The main parameters of the cone-driven ERG, including maximum amplitude and sensitivity, were in general agreement between WT and Trα $-/-$ animals (Table 1). Thus, we conclude that the ERG of the Trα $-/-$ mouse originated exclusively from cone-driven neurons that were present in their normal retinal densities. However, the Trα $-/-$ ERGs did exhibit a slower time to peak for responses of low to intermediate amplitude, particularly at UV wavelengths (Fig. 3*C*), suggesting some alteration in the signaling of light by cones or by cone-driven neurons.

Phototransduction in single cells was evaluated by suction-electrode recording. The vast majority of Trα $-/-$ rods (213 rods from four mice) failed to respond to flashes at 500 nm that delivered 600 times the number of photons required for a half-maximal response in a WT rod. Surprisingly, one cell did respond (Fig. 4*A*, *Bottom*) even though 24 other cells from the same mouse did not. The time to peak and the integration time of the dim-flash response in the responsive Trα $-/-$ cell were roughly twice as great as in WT rods (Fig. 4; Table 2). Whereas the WT response recovery exhibited a long-lasting tail after bright, saturating flashes, response recoveries of the responsive Trα $-/-$ cell had long tails even after subsaturating flashes. Furthermore, flash sensitivity of this Trα $-/-$ cell was more than 20 times lower, and the response amplitude increased with flash strength more gradually than in WT rods (Fig. 4*B*). The saturation time of the bright-flash response increased linearly with the natural logarithm of the flash strength for the responsive Trα $-/-$ cell and for WT rods. Although the relationship in the Trα $-/-$ cell was shifted to higher-flash strengths because of the cell's lower sensitivity, the slope was similar to that in WT rods (Fig. 4*C*; Table 2). With the exception of a slightly elevated sensitivity in the UV, the spectrum of the responsive Trα $-/-$ cell was indistinguishable from that of WT rods and from difference spectra of murine rhodopsin extracts (Fig. 4 *D* and *E*).

Flash responses of Trα $+/-$ rods were very similar to those of controls, although mean sensitivity tended to be lower (Fig. 4 *A–C*; Table 2). Trα $+/-$ rods did show an unusually high variance in sensitivity ($P < 0.00006$) compared with WT rods, perhaps because there were individual differences in the transducin content across Trα $+/-$ mice.

Discussion

The absence of a measurable a-wave in dark-adapted Trα $-/-$ mice and the failure of nearly every cell recorded individually to respond to flashes demonstrated that the overwhelming majority of rods required Trα for phototransduction. Unexpectedly, photoresponses were observed in one Trα $-/-$ cell. Perhaps phototransduction in a small population of rods can be supported by a G protein other than or in addition to Trα. For comparison, taste receptors use both transducin and gustducin, and deletion of gustducin impaired but did not eliminate sensitivity to bitter and sweet tastants (24). Alternatively, Trα knockout may have induced some rods to express a substitute G protein. About 3% of the photoreceptors in the mouse retina are cones that resemble rods at the light-microscopic level (25). However, UV- and mid-wavelength-sensitive cones have spectral maxima at 355–359 nm and 508–511 nm, respectively (16, 26, 27), whereas the murine rod is maximally sensitive at 502–503 nm. Also, mammalian rods express only a single type of pigment, but at least some cones contain a pigment mixture (16, 28). The spectral maximum for the responsive Trα $-/-$ cell was 503 nm, but sensitivity was somewhat high at short wavelengths, as would be expected for a cell that had UV-sensitive pigment in addition to rhodopsin (Fig. 4*D*). Hence, this cell may represent a previously uncharacterized photoreceptor type that was missed previously, because its members were too sparse to contribute significantly to the photopic-flash ERG (16), and their response kinetics were too slow to be detected by photopic-flicker methods (26). Consistent with this interpretation, some squirrel photoreceptors label with an antibody against rhodopsin, as well as by an antibody that recognizes short-wavelength-sensitive cone pigment, whereas other photoreceptors label with only one of the two antibodies (29).

It has been proposed that an inability to carry out sensory transduction is lethal to sensory neurons (30). Deletion of Goα in the accessory olfactory bulb disrupts olfactory transduction and causes postnatal apoptosis of the primary sensory neurons (30). Null mutations in rhodopsin (31–33) or in the cyclic-nucleotide-gated channel (34, 35) cause the progressive loss of the photoreceptors. In contrast, knockout of Trα precluded phototransduction, but few rods were lost. Parallel conditions exist in *Drosophila*, where greatly reduced levels of any of the

Table 1. ERG parameters

Type	b_{max}, μV	Sensitivity: 357 nm (photons$^{-1}\cdot\mu$m^2)	Sensitivity: 513 nm (photons$^{-1}\cdot\mu$m^2)	Sensitivity ratio 357/513
WT background	98 $\pm$ 16, 6	(1.7 $\pm$ 0.5) $\times$ 10^{-4}, 6	(3.0 $\pm$ 0.9) $\times$ 10^{-4}, 6	5.2 $\pm$ 0.5, 6
Tr$\alpha-/-$	120 $\pm$ 11, 9	(1.9 $\pm$ 0.5) $\times$ 10^{-4}, 5	(6.8 $\pm$ 1.2) $\times$ 10^{-4}, 5	3.0 $\pm$ 0.8, 5
Tr$\alpha-/-$ background	119 $\pm$ 13, 5	(1.1 $\pm$ 0.1) $\times$ 10^{-4}, 5	(3.4 $\pm$ 0.4) $\times$ 10^{-4}, 5	3.5 $\pm$ 0.4, 5

Values are means $\pm$ SEM, *n*. b_{max} is the maximal amplitude of the b-wave. Sensitivity is the fraction of the maximal b-wave response divided by the photon density at the cornea for responses in the linear range, i.e., $<0.3\ b_{max}$ (18). Background signifies continuous exposure to 540-nm light during the measurements.

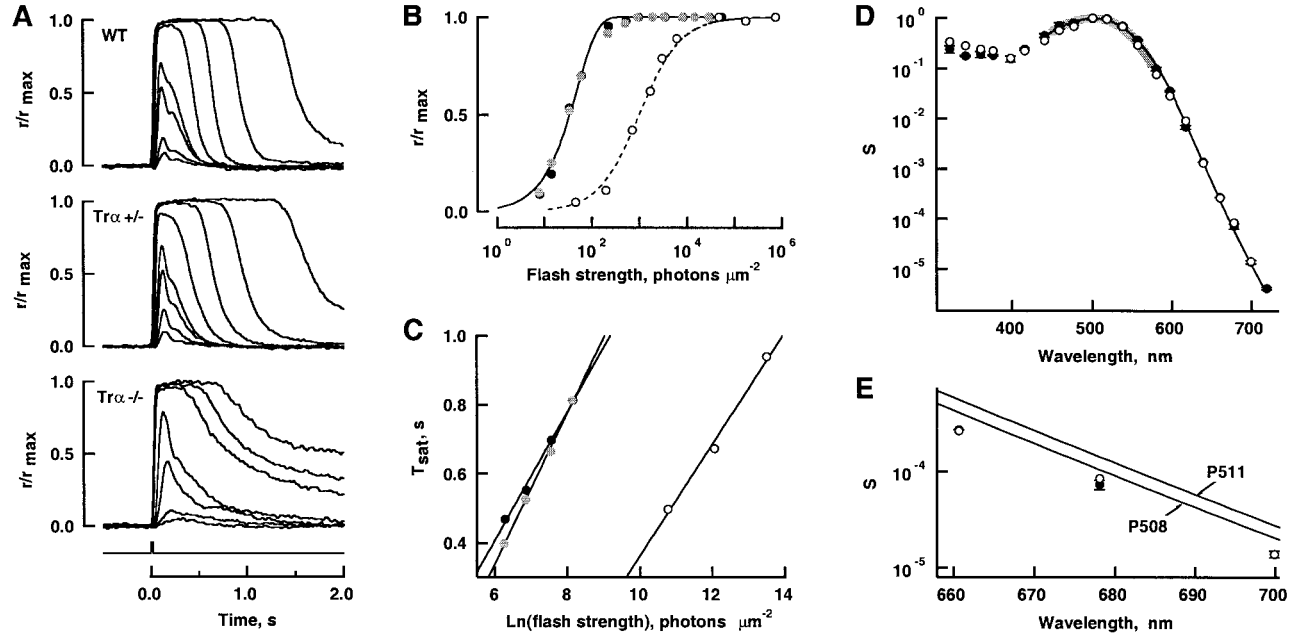

Fig. 4. Flash responses of single cells. (*A*) Averaged responses of WT, Trα +/−, and Trα −/− cells; maximal amplitudes were 9, 13, and 13 pA, respectively. Flash monitor is shown by the *Bottom* trace. (*B*) The stimulus-response relation for flashes at 500 nm for WT (●), Trα +/− (gray symbols), and Trα −/− (○) cells in *A*. Some traces were omitted in *A* for clarity. WT and Trα +/− results were fit with (continuous lines): $r/r_{max} = 1 - \exp(-ki)$, where i was flash strength, k was $\ln(2)/i_0$, and i_0 was the flash producing a half-maximal response. i_0 was 36 and 35 photons·μm^{-2} for WT and Trα +/−, respectively. Trα −/− results were fit with the Michaelis–Menten relation (broken line): $r/r_{max} = i/(i + i_0)$, where i_0 = 1,000 photons·μm^{-2}. (*C*) Recovery from response saturation. Saturation time (T_{sat}) was measured from midflash to 0.8 r_{max} on the falling phase of the saturated responses in *A*. A linear fit of T_{sat} to the natural logarithms of the flash intensities yielded the slopes: 0.186, 0.217, and 0.162 s for WT, Trα +/−, and Trα −/−, respectively. (*D*) Spectral sensitivities of four WT rods (●) and the responsive Trα −/− cell (○). The mean relative sensitivity and standard error at each wavelength were computed from the log S(λ) values. The fit of collected results with: $S(\lambda) = \{\exp[70(0.88 - \lambda_{max}/\lambda)] + \exp[28.5(0.924 - \lambda_{max}/\lambda)] + \exp[-14.1(1.104 - \lambda_{max}/\lambda)] + 0.655\}^{-1}$ (thin black line; ref. 23), weighted by $S(\lambda)^{-1}$, yielded a λ_{max} of 503 nm. The difference spectrum of rhodopsin extracted from WT retinas had a maximum at 502 nm (thick gray line). (*E*) The spectral sensitivity from *D* on expanded axes. The two continuous lines show spectra predicted for pigments with maxima at 508 and 511 nm.

three transducin subunit homologs caused sensitivity to fall by 2–3 log units but did not result in retinal degeneration (C.S. Zuker, personal communication). It may be that the absence of an outer segment in rods devoid of rhodopsin (32, 33) or the lack of functional channels hyperpolarized the rod, producing a state equivalent to that caused by continuous exposure to light. Excessive illumination is known to cause rods to degenerate (ref. 36; see ref. 37 for recent survey). Transducin is found throughout the photoreceptor, suggesting that it subserves a role in other signal-transduction pathways (38). These pathways must not be essential for rod viability. In sum, neither the presence of Trα nor the ability to phototransduce is necessary for rod survival. Furthermore, the presence of approximately normal UV- and mid-wave-sensitive cone-driven components in the ERG of Trα −/− mice establishes that retinal development and the formation of operational synapses were not seriously compromised by the absence of rod signaling.

Accordingly, deletion of Trα in humans would not be expected to cause retinitis pigmentosa. Instead, it could be the basis for a recessive stationary night blindness in which a-waves are absent from the ERG (39). Consistent with this prediction, the Nougaret form of stationary night blindness was traced to a mutation in Trα (40) that reportedly leaves transducin unable to activate PDE (41). The dominant transmission of Nougaret disease has not been explained, however. A genetic deletion of Tcα would be expected to result in achromatopsia or rod monochromacy. This condition is quite rare, and thus far, the few cases studied arose from mutations in the cone cGMP-gated channel (42) or in another protein of unknown function (43). If cones contain some Trα, then subtle cone abnormalities might be present in the absence of Trα, and partial cone function might be retained in the absence of Tcα.

Expressions of the rod transducin α- and β-subunits do not necessarily match. Levels of rod transducin β-subunit were unaffected by deletion of Trα (Fig. 1*E*) or by overexpression of a mutant Tcα (44). Flies deficient in Gβe maintained normal retinal levels of the α-subunit (45). It follows that free T$\beta\gamma$ should have been greatly increased in Trα −/− rods. In some

Table 2. Flash response parameters of single photoreceptors

Type	i_0, photons·μm^{-2}	Time to peak, ms	Integration time, ms	τ_c, ms
WT	55 ± 5, 14	131 ± 6, 12	209 ± 27, 12	213 ± 14, 9
Trα+/−	83 ± 12, 21	137 ± 3, 22	207 ± 12, 22	195 ± 14, 19
Trα−/−	1,000, 1	230, 1	530, 1	162, 1

Values are means ± SEM, *n*. i_0 is the flash strength at 500 nm producing a half-maximal response. Time to peak and integration time describe responses whose amplitudes were <0.2 r_{max} and fell within the linear range. Integration time is the area of the response divided by response amplitude. τ_c was given by the slope of the relation between response saturation time and the natural logarithm of the flash strength.

systems, the $\beta\gamma$-subunit of the G protein interacts with an effector (reviewed in ref. 46), but in rods, a role for T$\beta\gamma$ has not yet been defined. Rod T$\beta\gamma$ has been shown to stimulate phospholipase A2 in the retina (47); however, the physiological function of this pathway remains unknown. T$\beta\gamma$ will also bind to the soluble phosphoprotein, phosducin (48). Interestingly, phosducin was augmented in the Trα $-/-$ retina in a manner that might serve to prevent the accumulation of excess free T$\beta\gamma$.

It should be possible to rescue phototransduction in Trα $-/-$ rods by expressing Tcα or mutant forms of Tα and then test the biochemical properties of the resultant transducins in the intact cell. The Trα $-/-$ mouse also presents an opportunity for learning how the absence of rod input affects development and the processing of visual information in the proximal retina without the complications induced by massive rod degeneration. Because Trα is expressed in taste-receptor cells (49) and in the pineal, at least transiently during development (50), the Trα $-/-$ mouse could provide a means for studying alterations in taste and in extraretinal photoreception.

We thank S. Hagstrom and L. Fedorova for their invaluable assistance with the PCR analysis. Support was provided by the E. Mathilda Ziegler Foundation for the Blind to C.L.M.; the Research to Prevent Blindness: Career Development Awards to C.L.M. and J.L.; a Jules and Doris Stein Professorship to E.N.P.; National Institutes of Health Grants: EY11358 (to C.L.M.), EY06857 (to P.D.C.), EY02660 (to E.N.P), DC03055 (to R.F.M.), and P30 EY12196; the Foundation Fighting Blindness to J.L.; and the Massachusetts Lion's Eye Research Fund to C.L.M. and J.L. R.F.M. is an Associate Investigator of the Howard Hughes Medical Institute.

1. Roof, D. & Makino, C. L. (2000) in *Principles and Practice of Ophthalmology*, eds. Alberts, D. & Jakobiec, F. (Saunders, Philadelphia), 2nd Ed., Vol. 3., pp. 1624–1673.
2. Lerea, C. L., Somers, D. E., Hurley, J. B., Klock, I. B. & Bunt-Milam, A. H. (1986) *Science* **234,** 77–80.
3. Lerea, C. L., Bunt-Milam, A. H. & Hurley, J. B. (1989) *Neuron* **3,** 367–376.
4. Fung, B. K.-K., Lieberman, B. S. & Lee, R. H. (1992) *J. Biol. Chem.* **267,** 24782–24788.
5. Lee, R. H., Lieberman, B. S., Yamane, H. K., Bok, D. & Fung, B. K.-K. (1992) *J. Biol. Chem.* **267,** 24776–24781.
6. Peng, Y.-W., Robishaw, J. D., Levine, M. A. & Yau, K.-W. (1992) *Proc. Natl. Acad. Sci. USA* **89,** 10882–10886.
7. Ong, O. C., Yamane, H. K., Phan, K. B., Fong, H. K. W., Bok, D., Lee, R. H. & Fung, B. K.-K. (1995) *J. Biol. Chem.* **270,** 8495–8500.
8. Pronin, A. N. & Gautam, N. (1992) *Proc. Natl. Acad. Sci. USA* **89,** 6220–6224.
9. Schmidt, C. J., Thomas, T. C., Levine, M. A. & Neer, E. J. (1992) *J. Biol. Chem.* **267,** 13807–13810.
10. Kwee, L., Baldwin, H. S., Shen, H. M., Stewart, C. L., Buck, C., Buck, C. A. & Labow, M. A. (1995) *Development (Cambridge, U.K.)* **121,** 489–503.
11. Lem, J., Flannery, J. G., Li, T., Applebury, M. L., Farber, D. B. & Simon, M. I. (1992) *Proc. Natl. Acad. Sci. USA.* **89,** 4422–4426.
12. Wald, G. & Brown, P. K. (1953) *J. Gen. Physiol.* **37,** 189–200.
13. Witt, P. L., Hamm, H. E. & Bownds, M. D. (1984) *J. Gen. Physiol.* **84,** 251–263.
14. Lee, R. H., Whelan, J. P., Lolley, R. N. & McGinnis, J. F. (1988) *Exp. Eye Res.* **46,** 829–840.
15. Dizhoor, A. M., Ray, S., Kumar, S., Niemi, G., Spencer, M., Brolley, D., Walsh, K. A., Philipov, P. P., Hurley, J. B. & Stryer, L. (1991) *Science* **251,** 915–918.
16. Lyubarsky, A. L., Falsini, B., Pennesi, M. E., Valentini, P. & Pugh, E. N., Jr. (1999) *J. Neurosci.* **19,** 442–455.
17. Lyubarsky, A. L. & Pugh, E. N., Jr. (1996) *J. Neurosci.* **16,** 563–571.
18. Lyubarsky, A. L., Chen, C.-K., Simon, M. I. & Pugh, E. N., Jr. (2000) *J. Neurosci.* **20,** 2209–2217.
19. Sung, C.-H., Makino, C., Baylor, D. & Nathans, J. (1994) *J. Neurosci.* **14,** 5818–5833.
20. Pugh, E. N., Jr., Falsini, B. & Lyubarsky, A. L. (1998) in *Photostasis and Related Phenomena*, eds.. Williams, T. P. & Thistle, A. (Plenum, New York), pp. 93–128.
21. Robson, J. G. & Frishman, L. J. (1995) *Visual Neurosci.* **12,** 837–850.
22. Peachey, N. S., Goto, Y., Al-Ubaidi, M. R. & Naash, M. I. (1993) *Neurosci. Lett.* **162,** 9–11.
23. Lamb, T. D. (1995) *Vision Res.* **35,** 3083–3091.
24. Wong, G. T., Gannon, K. S. & Margolskee, R. F. (1996) *Nature (London)* **381,** 796–800.
25. Carter-Dawson, L. D. & LaVail, M. M. (1979) *J. Comp. Neurol.* **188,** 245–262.
26. Jacobs, G. H., Neitz, J. & Deegan, J. F., II (1991) *Nature (London)* **353,** 655–656.
27. Sun, H., Macke, J. P. & Nathans, J. (1997) *Proc. Natl. Acad. Sci. USA* **94,** 8860–8865.
28. Rohlich, P., van Veen, T. & Szel, A. (1994) *Neuron* **13,** 1159–1166.
29. Szel, A. & Rohlich, P. (1988) *Vision Res.* **28,** 1297–1302.
30. Tanaka, M., Treloar, H., Kalb, R. G., Greer, C. A. & Strittmatter, S. M. (1999) *Proc. Natl. Acad. Sci. USA* **96,** 14106–14111.
31. Rosenfeld, P. J., Cowley, G. S., McGee, T. L., Sandberg, M. A., Berson, E. L. & Dryja, T. P. (1992) *Nat. Genet.* **1,** 209–213.
32. Humphries, M. M., Rancourt, D., Farrar, G. J., Kenna, P., Hazel, M., Bush, R. A., Sieving, P. A., Sheils, D. M., McNally, N., Creighton, P., *et al.* (1997) *Nat. Genet.* **15,** 216–219.
33. Lem, J., Krasnoperova, N. V., Calvert, P. D., Kosaras, B., Cameron, D. A., Nicolo, M., Makino, C. L. & Sidman, R. L. (1999) *Proc. Natl. Acad. Sci. USA* **96,** 736–741.
34. Dryja, T. P., Finn, J. T., Peng, Y.-W., McGee, T. L., Berson, E. L. & Yau, K.-W. (1995) *Proc. Natl. Acad. Sci. USA* **92,** 10177–10181.
35. Biel, M., Seeliger, M., Pfeifer, A., Kohler, K., Gerstner, A., Ludwig, A., Jaissle, G., Fauser, S., Zrenner, E. & Hofmann, F. (1999) *Proc. Natl. Acad. Sci. USA* **96,** 7553–7557.
36. Noell, W. K., Walker, V. S., Kang, B. S. & Berman, S. (1966) *Invest. Ophthalmol.* **5,** 450–473.
37. Williams, T. P. & Thistle, A. B., eds. (1998) *Photostasis and Related Phenomena* (Plenum, New York).
38. Grunwald, G. B., Gierschik, P., Nirenberg, M. & Spiegel, A. (1986) *Science* **231,** 856–859.
39. Peachey, N. S., Fishman, G. A., Kilbride, P. E., Alexander, K. R., Keehan, K. M. & Derlacki, D. J. (1990) *Invest. Opthalmol. Visual Sci.* **31,** 237–246.
40. Dryja, T. P., Hahn, L. B., Reboul, T. & Arnaud, B. (1996) *Nat. Genet.* **13,** 358–360.
41. Muradov, K. G. & Artemyev, N. O. (2000) *J. Biol. Chem.* **275,** 6969–6974.
42. Kohl, S., Marx, T., Giddings, I., Jagle, H., Jacobson, S. G., Apfelstedt-Sylla, E., Zrenner, E., Sharpe, L. T. & Wissinger, B. (1998) *Nat. Genet.* **19,** 257–259.
43. Winick, J. D., Blundell, M. L., Galke, B. L., Salam, A. A., Leal, S. M. & Karayiorgou, M. (1999) *Am. J. Hum. Genet.* **64,** 1679–1685.
44. Raport, C. J., Lem, J., Makino, C., Chen, C.-K., Fitch, C. L., Hobson, A., Baylor, D., Simon, M. I. & Hurley, J. B. (1994) *Invest. Ophthalmol. Visual Sci.* **35,** 2932–2947.
45. Dolph, P. J., Man-Son-Hing, H., Yarfitz, S., Colley, N. J., Running Deer, J., Spencer, M., Hurley, J. B. & Zuker, C. S. (1994) *Nature (London)* **370,** 59–61.
46. Clapham, D. E. & Neer, E. J. (1997) *Annu. Rev. Pharmacol. Toxicol.* **37,** 167–203.
47. Jelsema, C. L. & Axelrod, J. (1987) *Proc. Natl. Acad. Sci. USA* **84,** 3623–3627.
48. Lee, R. H., Lieberman, B. S. & Lolley, R. N. (1987) *Biochemistry* **26,** 3983–3990.
49. Ruiz-Avila, L., McLaughlin, S. K., Wildman, D., McKinnon, P. J., Robichon, A., Spickofsky, N. & Margolskee, R. F. (1995) *Nature (London)* **376,** 80–85.
50. Blackshaw, S. & Snyder, S. H. (1997) *J. Neurosci.* **17,** 8074–8082.